Effects of Load Sequence and Block Loading on the Fatigue Response of Fibre-reinforced Composites

W. VAN PAEPEGEM
J. DEGRIECK

Ghent University, Dept. of Mechanical Construction and Production,
Sint-Pietersnieuwstraat 41, 9000 Gent, Belgium

ABSTRACT

The vast majority of fatigue loading experiments are constant amplitude tests, although this type of fatigue loading is hardly present in real in-service fatigue loading conditions. However, due to the expensive and time-consuming nature of variable amplitude experiments, their effect is often assessed by performing block loading experiments with various low-high and high-low sequences. In this paper, the effects of load sequence and block loading on the fatigue damage development in fibre-reinforced polymer composites will be investigated. First it will be shown that the opinions in open literature on the damaging effect of low-high and high-low load sequences are divided. Next the effect of block loading on the bending fatigue behaviour of composites will be experimentally tested and numerically simulated with a newly developed fatigue damage model. Finally numerical simulations will show that the transitions from low to high stress levels are the most damaging, and that the number of transitions and their relative importance in particular determine which block loading sequence (low-high or high-low) is the most devastating.

In studying the fatigue behaviour of fibre-reinforced composites, it is of course best to simulate the in-service fatigue loading conditions as nearly as possible. In the mechanical load-time history acting on a component in service, loading is virtually always of variable amplitude and only rarely of constant amplitude. Nevertheless, fatigue testing is still being carried out under constant amplitude, this choice being dictated largely by the expensive and time-consuming nature of the variable amplitude experiments, the limitations of standard fatigue testing facilities and the uncertainties about the in-service loading spectrum [1].

When the results of constant amplitude fatigue tests are to be extrapolated towards variable amplitude fatigue loading, "damage accumulation rules" or "cumulative damage laws" must be used. The simplest of these is the well known Palmgren-Miner rule [2]:

$$D = \sum \frac{n_i}{N_{fi}} \qquad (1)$$

where D denotes the fatigue damage, and n_i and N_{fi} are the number of actually applied cycles and the total number of cycles to failure for the i-th constant amplitude loading level, respectively. At failure, D = 1 and n = N_f. This rule is a linear damage accumulation rule which was originally proposed for the life prediction of metallic components undergoing fatigue, and, despite its widespread use, the rule has always been viewed with great suspicion by designers because it is often found to give non-conservative results: that is, to predict lives greater than those observed experimentally [3]. Its main deficiencies are: (i) load level independence, (ii) load sequence independence, and (iii) lack of load interaction accountability [4].

The simplest step forward from the linear damage rule is to look for non-linear functions that still employ the damage parameter D, as defined by Eq. (1). In the Marco-Starkey model, for example, a simple non-linear presentation suggests an equation of the form:

$$D = \sum \left(\frac{n_i}{N_{fi}} \right)^{\alpha} \qquad (2)$$

where the power α is a load-dependent variable. Life calculations based on the Marco-Starkey theory result in a Miner's sum $\sum \left(n_i / N_{fi} \right) > 1$ for low-high load sequences, and in a Miner's sum $\sum \left(n_i / N_{fi} \right) < 1$ for high-low load sequences [4].

The different life predictions for low-high and high-low load sequences correspond to the experimentally observed "load sequence effect": a different fatigue life of metallic or composite components under low-high and high-low load sequences.

The load sequence effect is often investigated by performing block loading fatigue experiments. This effect will now be discussed in detail for fibre-reinforced composite materials. First a literature survey will show that there is no agreement at all in open literature which sequence (low-high or high-low) is the most disastrous for composites. Next the effect of block loading on the fatigue response of composites will be investigated by experimental results and numerical simulations with a newly developed fatigue damage model. Finally numerical simulations will show that, in the authors' opinion, the most damaging effect is in the (frequent) transition from low to high stress levels. The proposed fatigue damage model will lead to new insights into how cumulative damage should be treated.

LITERATURE SURVEY ON LOAD SEQUENCE EFFECTS AND BLOCK LOADING

To investigate the load sequence effect, block loading experiments are the most commonly used experiments. Cycle blocks with constant load amplitude level are imposed and the effect of their sequence on the fatigue life of the composite component is investigated.

The cumulative damage under subsequent block loadings is usually evaluated using residual life theory or residual strength theory [5]. In the residual life theory, the damage D is a function of the elapsed number of cycles n_i and the number of cycles to failure N_{fi} for a given constant maximum amplitude σ_i : $D(n_i, N_{fi})$. The simplest example of such a damage function is the Palmgren-Miner rule (see Eq. (1)). The "damage equivalence" principle is then used to determine the number of cycles n_2, which produce at stress amplitude σ_2 the same damage as n_1 cycles at stress amplitude σ_1 [5]:

$$D(n_1, N_{f1}) = D(n_2, N_{f2}) \qquad (3)$$

In the residual strength theory on the other hand, the damage function D can be written as $D(\sigma_i, \sigma_r)$, where σ_i is the applied constant amplitude stress level and σ_r is the residual strength. The variables σ_i and σ_r are related to the elapsed number of cycles n_i and the number of cycles to failure N_{fi} by the S-N curve and the residual strength model. Again, the principle of damage equivalence is applied for two-stage loading:

$$D(\sigma_1, \sigma_{r1}) = D(\sigma_2, \sigma_{r2}) \qquad\qquad (4)$$

Hashin [5] has shown that the residual life and residual strength cumulative damage theories are completely equivalent since an assumed functional form of residual strength curves determines a damage function and thus the residual life.

Such cumulative damage theories are then used to assess the fatigue life under block loading and spectrum loading. When studying the literature about this subject, there is only one general conclusion to be drawn: there is no agreement at all which load sequences have the worst effect on fatigue life. For example, in 1998, Bartley-Cho et al. [6] wrote: "*For composites, these tests reveal a load sequence effect where a low-high loading sequence results in a shorter fatigue life than a high-low loading sequence*". In 2000, Gamstedt and Sjögren [7] claimed: "*In an experimental investigation, the interaction of these mechanisms has shown why a sequence of high-low amplitude level results in shorter life-times than a low-high order*". Of course, both opinions are always based on experimental observations, but unfortunately with different materials, different loading conditions and different applied stress levels, so that a decision in favour of one of the both opinions is difficult to make. Here, the classification of the representative publications of each opinion has been based on the outcome of the experimental results against which the cumulative damage models have been validated.

Fatigue life L-H < Fatigue life H-L

Almost all evaluations of cumulative damage models in this category use the data of Broutman and Sahu [8], who performed block loading fatigue tests on cross-ply E-glass/epoxy specimens. All of these fatigue tests were performed at 10 Hz with a stress ratio R of 0.05. The average value of the ultimate static strength was given as 448 MPa. They observed that in general, a low-high sequence was more damaging than a high-low sequence.

Yang and Jones [9] developed a residual strength model where the static ultimate strength is assumed to follow a two-parameter Weibull distribution. As a consequence, the predicted fatigue life is a statistical variable as well, presented by a three-parameter Weibull-distribution. Based on these statistical distributions, it was derived that the Miner's sum D is always greater than unity under the high-low loading sequence and always smaller than unity under the low-high loading sequence [9]. Of course, the validity of this statement depends on the correctness of the residual strength model proposed.

Further, Yang and Jones [9] proposed to replace the Miner's sum by the residual strength concept, where it is assumed that the residual strength $R(n_1)$ after n_1 cycles (stress σ_1) can be considered as the initial strength for subsequent cycling at stress amplitude σ_2. The theory was applied to block loading experiments of cross-ply E-glass/epoxy specimens, performed earlier by Broutman and Sahu [8]. Hashin [5] compared the residual strength approach of Yang and Jones, amongst others, with the Palmgren-Miner rule, and concluded that none of the residual strength models gives a better fatigue life prediction than the simple Palmgren-Miner rule.

Schaff and Davidson [10,11] adopted the same principle of residual strength equivalence to extend their residual strength model to multi-stress level loadings. However, they additionally introduced a so-called "cycle mix factor". This factor should account for the damaging effect

of frequent transitions from low to high mean stress. This "cycle mix effect" was described in detail by Farrow [12] and means that the residual strength and the fatigue life of composite laminates had been observed to decrease more rapidly when the loading sequence is repeatedly changed after only a few loading cycles. Again the data provided by Broutman and Sahu [8] were used to validate their cumulative damage model.

Whitworth [13] derived a non-linear cumulative damage law which is in fact a modified form of the Palmgren-Miner sum, by introducing a stress-dependent factor into the expression. He applied the rule to experimental data of tension fatigue tests (R = 0.1) on graphite/epoxy laminates. Again, the low-high load sequence resulted in shorter fatigue lives than the high-low load sequence in correspondence with the experimental results.

Bartley-Cho et al. [6] performed two-block loading fatigue tests on quasi-isotropic graphite/epoxy laminates. They observed that a low-high sequence resulted in higher crack densities than a high-low sequence. However their cumulative damage model was load-history independent and did not manage to simulate these experimentally observed results.

Lee and Jen [14,15] recently proposed a non-linear damage accumulation rule which is based on the Marco-Starkey cumulative damage law (see Eq. (2)) and validated their model against the results reported by Broutman and Sahu [8].

Fatigue life L-H > Fatigue life H-L

Hwang and Han [16] mentioned in their review about cumulative damage models that *"… it is a generally known fact that the Palmgren-Miner's damage sum to failure is greater than unity for low-high tests and less than unity for high-low tests"*. Their statement was based on the experimental results by Han and Hamdi [17], who performed tension fatigue tests on glass fiber cloth epoxy composites. These results indeed showed that low-high tests were more beneficial than high-low tests.

Adam et al. [3,18] proposed a residual life cumulative damage theory, where the power α in the Marco-Starkey model (see Eq. (2)) is a stress-dependent function, but this function is now different for tension and compression loading. The model was applied to four-unit block loading sequences for carbon/epoxy laminates. It was concluded that a lower initial stress appears to be more beneficial than a higher initial stress.

Gamstedt and Sjögren [7] observed that for cross-ply carbon/epoxy laminates, a sequence of high-low amplitude levels resulted in shorter lifetimes than a low-high order. They state that initiatory mechanisms are active at high stress levels, and that progressive mechanisms predominate at lower amplitudes. As a high-low sequence gives rise to damage from which the progressive mechanisms can start, it is more damaging than the low-high sequence.

It can be concluded from the literature review that the opinions are strongly divided. Moreover it is very difficult to assess the generality of these experimental observations, because different materials, lay-ups and block loading conditions have been used in each experimental workplan.

In the next paragraph, the fatigue damage model, developed by the authors, will be presented. This phenomenological residual stiffness model aims at modelling the underlying fatigue damage mechanisms and at predicting the damage growth during fatigue life. This model will then be used to simulate block loading experiments and to investigate the load sequence effect.

LAYOUT OF THE FATIGUE DAMAGE MODEL

Recently, the authors proposed a new fatigue damage model that is capable of simulating the three stages in stiffness degradation (sharp initial decline – gradual deterioration – final failure) [19]. This phenomenological model is valid for uni-axial loading of delamination-free specimens with zero stress-ratio $R = \sigma_{min}/\sigma_{max}$.

The model is based on the residual stiffness approach. Hence stress and strain are related by the commonly used equation in continuum damage mechanics:

$$\tilde{\sigma} = \frac{\sigma}{1-D} = E_0 \varepsilon \tag{5}$$

where $\tilde{\sigma}$ is the effective stress, σ is the applied nominal stress, ε is the nominal strain, E_0 is the undamaged Young's modulus and D ($= 1 - E/E_0$) is a measure for the fatigue damage. Its value is lying between zero (virgin material state) and one (final failure).

The main drawback of the residual stiffness models is that they do not provide a means to estimate the moment of final failure. This problem is solved by establishing a relation between the damage variable D (measure for the residual stiffness) and a "fatigue failure index". Thereto, the Tsai-Wu static failure criterion is interpreted in a different manner. The effective stress $\tilde{\sigma}$ is inserted in the Tsai-Wu criterion and the reserve factor R to failure is calculated from the Tsai-Wu equation:

$$\left[\left(\frac{\sigma}{1-D} \right)^2 \frac{1}{X_T \cdot |X_C|} \right] R^2 + \left[\frac{\sigma}{1-D} \left(\frac{1}{X_T} - \frac{1}{|X_C|} \right) \right] R - 1 = 0 \tag{6}$$

where X_T and X_C are the static tensile and compressive strength, respectively. The fatigue failure index $\Sigma(\sigma, D)$ is then defined as the inverse of the reserve factor R. Hence the fatigue failure index is the ratio of the applied effective stress $\tilde{\sigma}$ to the static strength; it has a value between zero (applied stress equals zero) and one (effective stress equals static strength). This measure for the applied stress in relation to the static strength is now used in the damage growth rate equation dD/dN that is given by [19]:

$$\frac{dD}{dN} = \begin{vmatrix} c_1 \cdot \Sigma \cdot \exp\left(-c_2 \frac{D}{\sqrt{\Sigma}} \right) + c_3 \cdot D \cdot \Sigma^2 \cdot \left[1 + \exp\left(c_5 (\Sigma - c_4) \right) \right] & \text{if } \sigma \geq 0 \\ \left[c_1 \cdot \Sigma \cdot \exp\left(-c_2 \frac{D}{\sqrt{\Sigma}} \right) \right]^3 + c_3 \cdot D \cdot \Sigma^2 \cdot \left[1 + \exp\left(\frac{c_5}{3} (\Sigma - c_4) \right) \right] & \text{if } \sigma < 0 \end{vmatrix} \tag{7}$$

The growth rate is different in tension and compression, because it has been observed from the experimental fatigue tests that compressive damage growth rate is much smaller under the following restrictive conditions: (i) the stress ratio R is positive or zero for all the material points involved, and (ii) there are no delaminations.

In the damage growth rate equations, all five constants c_i (i = 1,…, 5) have a distinctive meaning:
- c_1 regulates the growth rate of the damage initiation regime (and thus the sharp initial decline of the modulus degradation curve),
- c_2 is sufficiently large, so that the first term disappears when damage increases. Then the steady state of matrix cracking, the so-called "Characteristic Damage State" [20-22] has been reached,

- c_3 represents the growth rate in the second stage of modulus degradation. Additional damage mechanisms (fibre/matrix debonding, pull-out from fibres out of the matrix, initial fibre breakage,…) are developing gradually in this stage of fatigue life,
- c_4 and c_5 express the explosive damage growth once that the failure index $\Sigma(\sigma, D)$ approaches its failure value 1.0 and the effective stress $\tilde{\sigma}$ approaches the static strength in tension or compression. When the threshold c_4 has been crossed, fibre fracture starts to propagate and finally causes failure in that material point.

MATERIALS AND EXPERIMENTAL SETUP

The material used in the fatigue experiments, was a glass fabric/epoxy composite. The fabric was a Roviglass R420 plain woven glass fabric (Syncoglas) and the epoxy was Araldite LY 556 (Ciba-Geigy). The plain woven glass fabric was stacked in eight layers, denoted as $[\#0°]_8$, where '0°' means that the warp direction of each of the eight layers has been aligned with the loading direction and where the symbol '#' refers to the fabric reinforcement type. All composite specimens were manufactured using the resin-transfer-moulding technique. After curing they had a thickness of 2.72 mm. The samples were cut to dimensions of 145 mm long by 30 mm wide on a water-cooled diamond saw. The fibre volume fraction V_f was 0.48.

The experimental results were obtained from displacement-controlled cantilever bending fatigue experiments. One side of the specimen was clamped, while a sinusoidal displacement was imposed at the other side of the specimen. Figure 1 shows a schematic drawing.
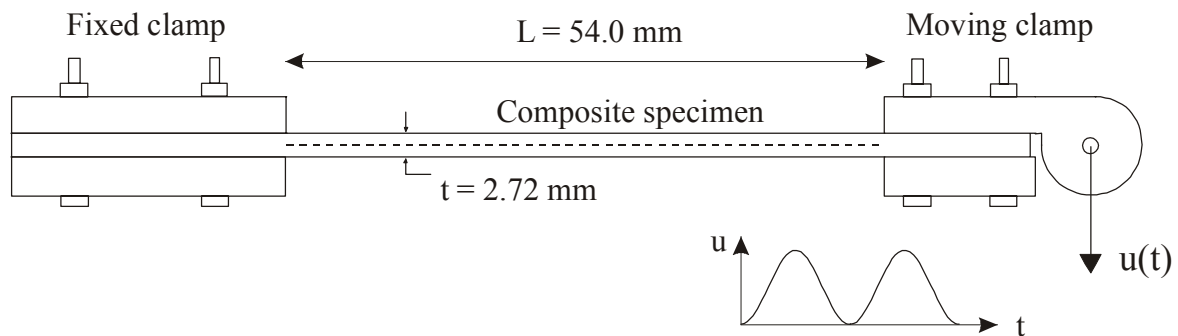
**Figure 1**   **Schematic drawing of the bending fatigue setup.**

The amplitude u_{max} of the imposed displacement is a controllable parameter and the displacement ratio R_d (analogous to the stress ratio R) is defined as $R_d = u_{min}/u_{max}$. For single-sided bending the displacement ratio $R_d = 0.0$, which means also that the stress ratio R is zero for each point in the structure. Of course, due to the varying bending moment along the specimen length and the varying stresses and strains along the specimen length and through its thickness, the maximum stress amplitude can be different in each point.

FINITE ELEMENT SIMULATIONS

The fatigue damage model (Eq. (7)) has been implemented in the commercial finite element code SAMCEF^{TM}. The integration of the damage growth rate equation for each Gaussian point of the finite element mesh has been done with the *cycle jump* approach which has been

recently proposed by the authors [23]. Briefly the *cycle jump* approach means that the computation is done for a certain set of loading cycles at deliberately chosen intervals, and that the effect on the stiffness degradation of these loading cycles is extrapolated for each Gaussian point over the corresponding intervals in an appropriate manner.

The parameters c_i (i=1,…,5) in Eq. (7) were determined for a "standard" experiment. Since the fatigue damage model is not at all a curve-fitting model, the value of the constants c_i (i=1,…,5) were of course retained when simulating other loading conditions. Figure 2 shows the experimental and the simulated force-cycle history for the fatigue test "Pr05_2". The imposed displacement varied between zero (stress ratio R = 0 for all Gaussian points) and u_{max} = 30.4 mm, and the frequency was 2.2 Hz. The force was experimentally measured by a strain gauge bridge and represents the force necessary to impose the bending displacement with constant amplitude u_{max}. Due to the (bending) stiffness degradation, this force will decrease during fatigue life.
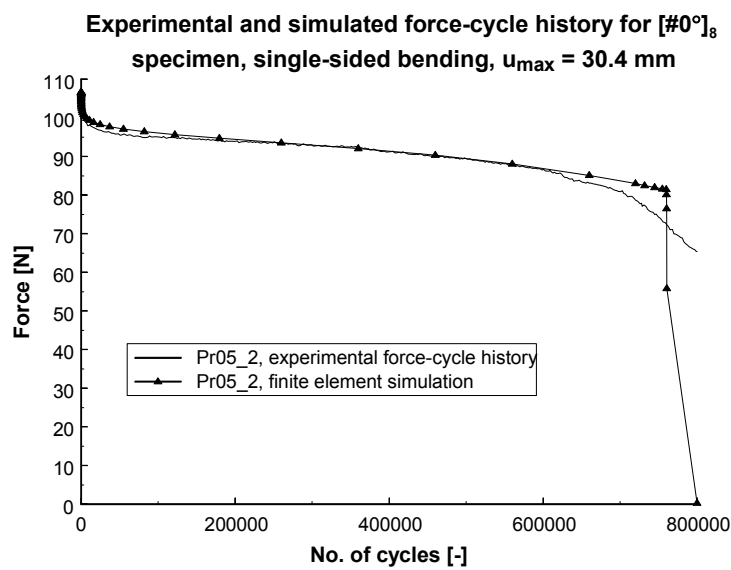
Figure 2   **Experimental and simulated force-cycle history.**

The parameters were optimized with a non-linear optimization procedure. The final values of all constants in the model are listed in Table 1. The in-plane elastic properties of the $[\#0°]_8$ composite laminates were determined using the dynamic modal analyis method described by Sol et al. [24,25], while the static strength values were determined with an Instron hydraulic testing machine.

Table 1   **Material and model constants.**

| Material parameters		Model parameters	
E_{11} [GPa]	24.57	c_1 [1/cycle]	0.002
E_{22} [GPa]	23.94	c_2 [-]	30.0
ν_{12} [-]	0.153	c_3 [1/cycle]	$4.0 \cdot 10^{-6}$
G_{12} [GPa]	4.83	c_4 [-]	0.85
X_T [MPa]	390.7	c_5 [-]	93.0

X_C [MPa]	345.1

Now the fatigue damage model is applied to a block loading fatigue experiment. First a block of 766,000 cycles with a small displacement $u_{max} = 7.1$ mm is applied, next a second block with a larger displacement $u_{max} = 29.5$ mm is applied until final failure. All model constants (Table 1) are retained. The experimental and simulated results are shown in Figure 3.

Degradation of [#0°]$_8$ specimen with small and large displacement
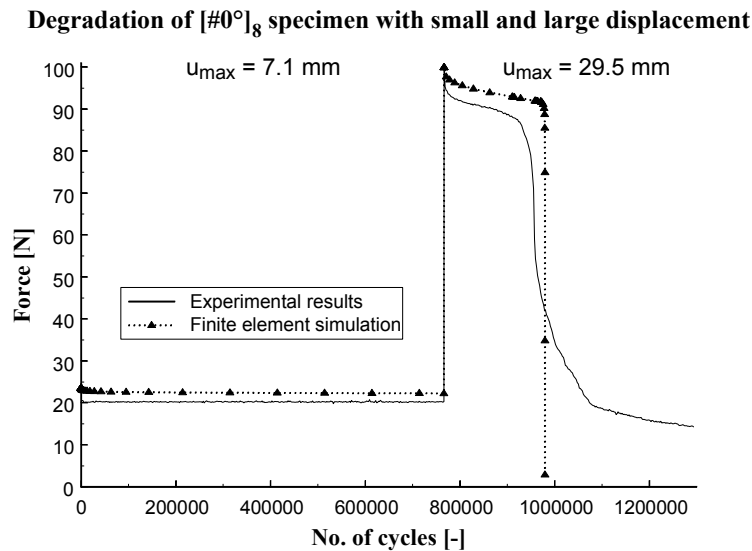
Figure 3   Block loading experiment with small and large displacement block.

The initial force for the small displacement is somewhat higher than the experimentally measured force. This is due to the slightly non-linear behaviour of the stress-strain response.
At approximately one million cycles, the bending stiffness of the composite specimen reduces to nearly zero and a sort of "hinge" is formed at the clamped cross-section. This means that the remaining life under the second block was about 200,000 cycles, while it was shown in the experiment and the simulation of Figure 2 that the fatigue life without "pre-loading" was more than 700,000 cycles for an even larger displacement $u_{max} = 30.4$ mm. It appears that the fatigue damage model can simulate the observed experimental behaviour very well, including the moment of failure, due to the use of the failure index $\Sigma(\sigma, D)$ (Eq. (6)).
In Figure 4, corresponding with the force-cycle history of Figure 3, the simulated stress redistribution during fatigue life is shown at the clamped cross-section. The abscissa contains the stress values, with tensile stresses being positive and compressive stresses being negative. The ordinate axis represents the full specimen thickness ($y \in$ [-1.36 mm, +1.36 mm]).

Stress distribution at the clamped cross-section
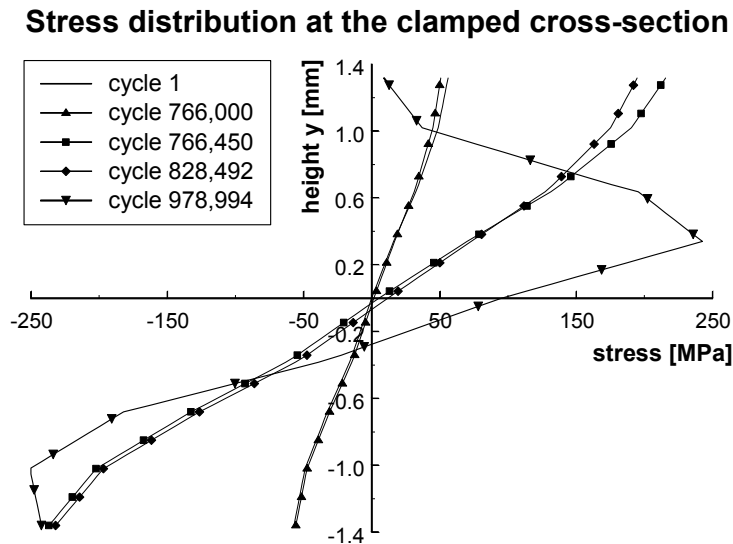
Figure 4   Stress redistribution during fatigue life at the clamped cross-section.

The first two curves show the stress distribution at the first loading cycle and at the last loading cycle before the second block was applied. The three last curves show the stress distribution at the first cycle of the second loading block, about 60,000 cycles later, and just before final failure. It is seen from the last curve that the tensile stress at the upper surface has exceeded the tensile strength X_T, hence the damage variable D equals 1.0 and the stiffness of that Gaussian point drops to zero.

It is important to note that these stress distributions are solely governed by the fatigue damage model. Each Gaussian point has been assigned a damage variable D (= $1 - E/E_0$) and the damage development for that particular Gaussian point is driven by the amplitude of the effective stress $\tilde{\sigma}$ (or equivalent: the failure index $\Sigma(\sigma, D)$) in that point. For each simulated loading cycle, the stress distribution in the composite component is then the equilibrium stress state under the imposed bending state u_{max}, while the stiffness (E = $E_0(1-D)$) can vary from point to point. Of course finite element simulations are indispensable to calculate these stress states at different stages during fatigue life.

LOAD SEQUENCE EFFECT: NUMERICAL SIMULATIONS

It will now be qualitatively demonstrated by numerical simulations that the damaging effect under block loading is due to transitions from low to high stress levels, and to the number of such transitions. Schaff and Davidson [10,11] already expressed the same opinion, but to model this damaging effect, they had to introduce a so-called "cycle mix factor" which was applied at each transition where the mean stress increased. Here, it will be shown that the fatigue damage model (Eq. (7)) can simulate these effects without any modification. Moreover, cumulative damage rules are needless, because the damage growth rate equation dD/dN is simply integrated over the various loading blocks.

Before simulating the block loading experiments, the fatigue life N_{fi} for certain constant amplitude stress levels σ_i (0.3, 0.4, 0.6 and 0.7 × X_T) is determined. In Table 2, the applied stress levels and the corresponding number of cycles to failure are listed.

**Table 2   Fatigue life for different constant amplitude stress levels in zero-tension fatigue.**

$\dfrac{\sigma_i}{X_T} (X_T = 390.7 \text{ MPa})$	Number of cycles to failure N_{fi}
0.3	1,533,400
0.4	695,220
0.6	107,326
0.7	22,220

Next a high-low and a low-high load sequence is simulated, where the second block is applied when the Palmgren-Miner's sum of the first block equals 0.5. Thus, for the high-low load sequence, 53,663 cycles at stress level $0.6 \times X_T$ are followed by a run-out at stress level $0.4 \times X_T$, while for the low-high load sequence, 347,610 cycles at stress level $0.4 \times X_T$ are followed by a run-out at stress level $0.6 \times X_T$. The damage evolution for both load sequences is shown in Figure 5.
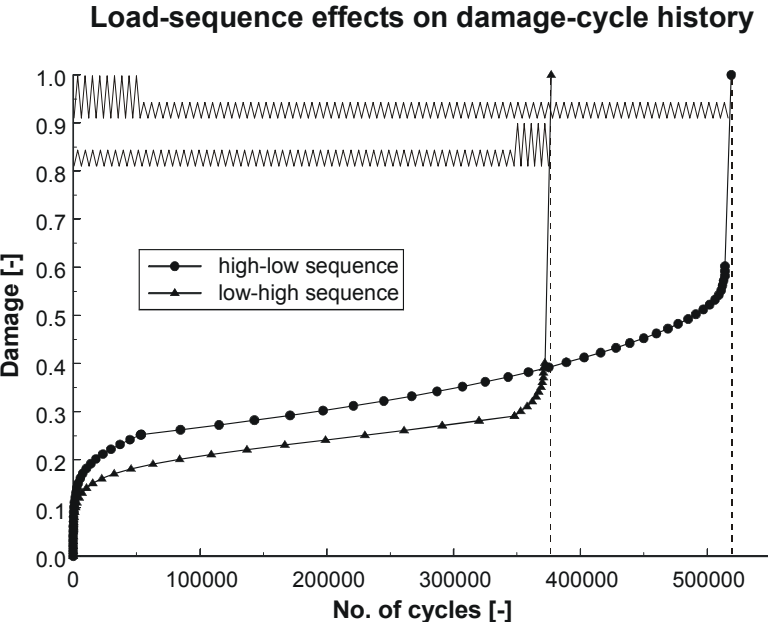
Figure 5   Damage-cycle history for high-low and low-high load sequences.

Failure is predicted at 376,660 cycles for the low-high load sequence and at 541,253 cycles for the high-low load sequence. The corresponding Miner's sum equals 0.77 and 1.162, respectively. In Figure 6 the cycle history of the failure index $\Sigma(\sigma, D)$ is shown for both load sequences.

Load-sequence effects on failure index-cycle history
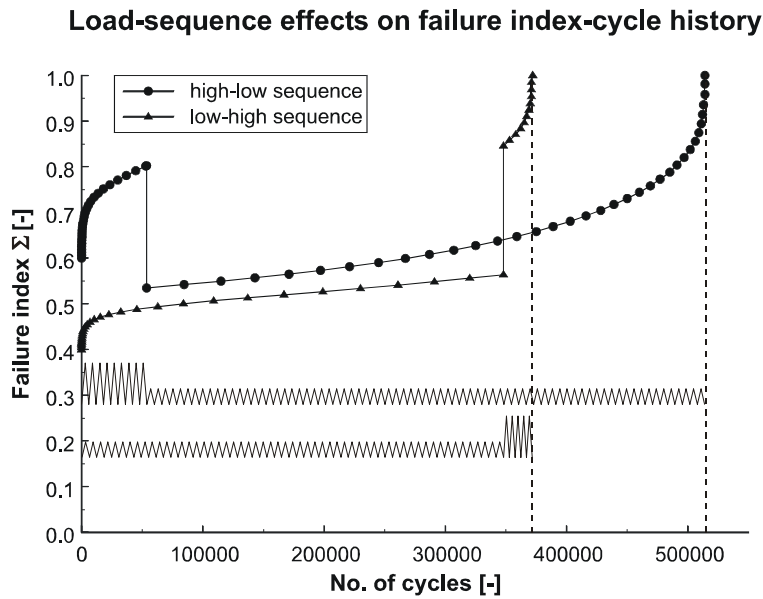
Figure 6 **Failure index-cycle history for high-low and low-high load sequences.**

The transition from a low stress level to a high stress level is here more damaging than from high to low, because when damage is already present, the effective stress $\widetilde{\sigma}$ (= $\sigma/(1-D)$) increases more than the applied nominal stress σ. For instance, after the low level block, the damage D equals 0.25, so when the stress σ is raised from $0.4 \times X_T$ to $0.6 \times X_T$, the failure index is not increased with 0.2, but with 0.266.

To simulate the "cycle mix effect", Schaff and Davidson [10,11] introduced a so-called "cycle mix factor", but as mentioned earlier, this is not necessary with the present fatigue damage model. Each time that the mean stress is increased, the effective stress and hence the failure index increases more than proportional, due to the division by the factor $(1 - D)$. As a consequence, the initiation term in Eq. (7) contributes each time that the mean stress is raised.

In Figure 7, the effect of "cycle mix loading" with small and large cycle blocks is shown. In the large cycle block loading, the low blocks ($0.4 \times X_T$) are 140,000 cycles in length, while the high blocks ($0.6 \times X_T$) are 20,000 cycles in length. In the small cycle block loading, the low blocks ($0.4 \times X_T$) are 35,000 cycles in length, while the high blocks ($0.6 \times X_T$) are 5,000 cycles in length.
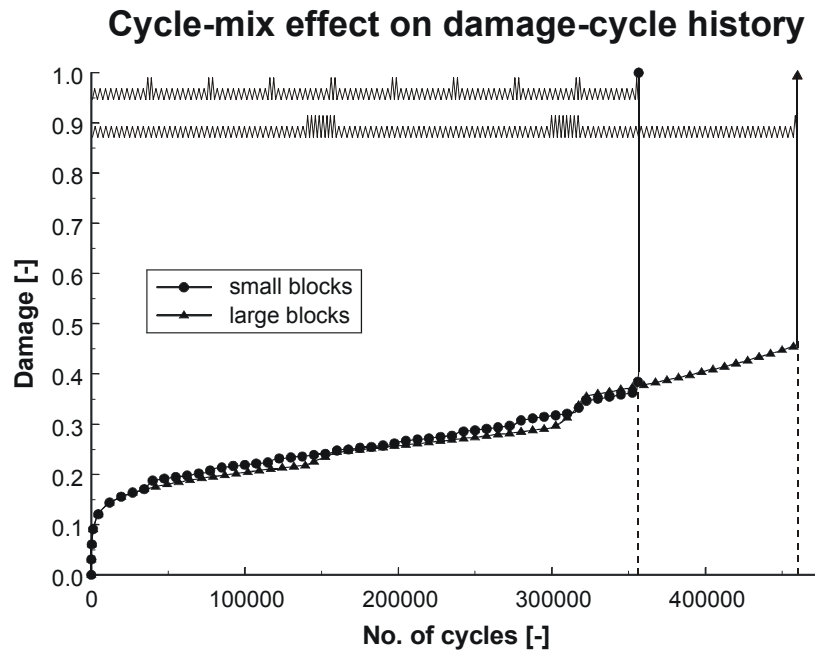
Figure 7   **Cycle-mix effect on the damage-cycle history.**

For the large cycle block loading, failure is predicted at 460,002 cycles, while for the small cycle block loading, failure occurs at 356,576 cycles, just at the moment when a new high cycle block has started. This can be explained by Figure 8, which shows the failure index-cycle history for the small cycle block loading. At the last transition from low to high stress level, the damage D equals 0.41 and the applied nominal stress raises from $0.4 \times X_T$ to $0.6 \times X_T$, but the failure index reaches its failure value 1.0, due to the much larger increase in effective stress.
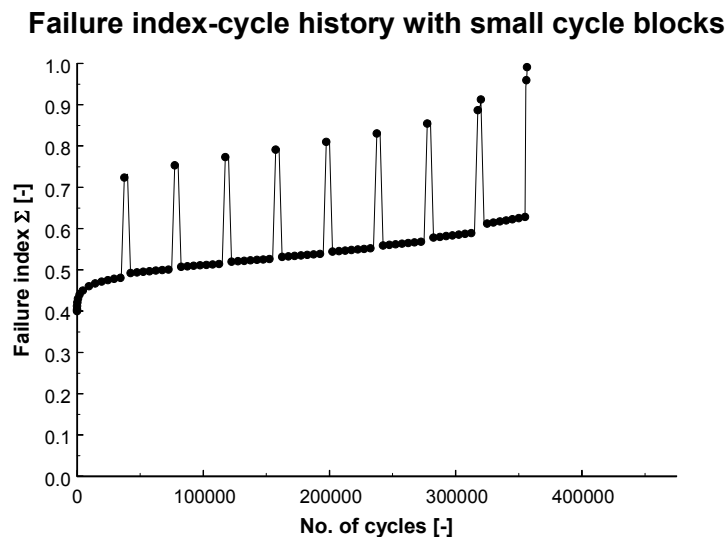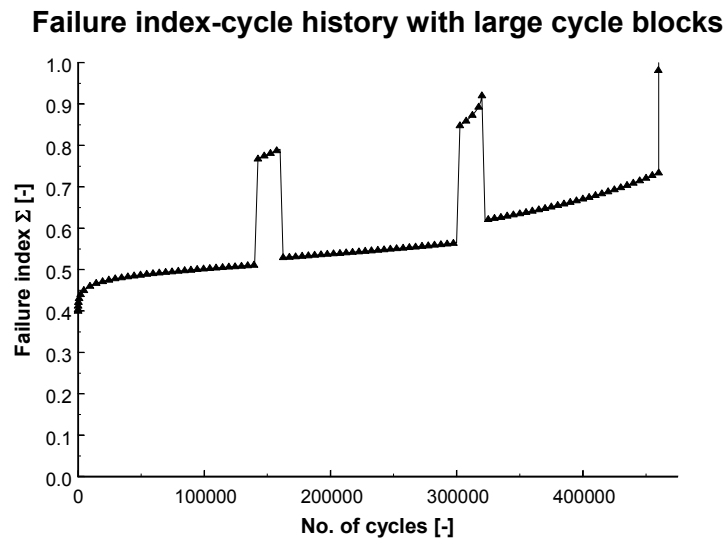

Figure 8   **Failure index-cycle history for the small cycle blocks of Figure 7.**

Figure 9 shows the failure index-cycle history for the large cycle block loading. Again, failure occurs at the last transition from low to high stress level.

Figure 9   Failure index-cycle history for the large cycle blocks of Figure 7.

The load sequence effect and the cycle mix effect have been simulated separately so far. From Figure 5, it could be concluded that a low-high sequence is more damaging than a high-low sequence. On the other hand, Adam et al. [3,18] concluded from their four-unit block loading experiments that a low initial stress appears more beneficial than a high initial stress. It will be qualitatively demonstrated by the numerical simulations that the conclusion of Figure 5 and the conclusion of Adam et al. [3] are not necessarily in contradiction with each other, because both the load sequence effect and the cycle mix effect are present in the four-unit block loading experiments. To that purpose, these experiments by Adam et al. [3,18] will be numerically simulated for the glass/epoxy material under study with the present fatigue damage law (Eq. (7)). The approach is almost exactly the same as followed by Adam et al.: four-unit blocks with respective stress levels of 0.3, 0.4, 0.6 and 0.7 × X_T are once applied in ascending order and once in descending order. The fractional life of each separate unit is 5 % ($= n_i / N_{fi}$), so that the Palmgren-Miner's sum of a complete four-unit block is 0.20. The data are summarized in Table 3.

Table 3   Four-unit block loading simulations.
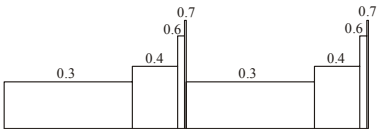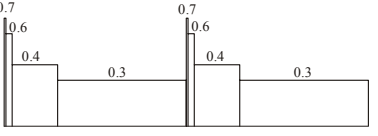
	Applied stress levels	Length cycle blocks	Miner's sum
(diagram)	$\sigma_1 = 0.3\,X_T = 117.2$ MPa $\sigma_2 = 0.4\,X_T = 156.3$ MPa $\sigma_3 = 0.6\,X_T = 234.4$ MPa $\sigma_4 = 0.7\,X_T = 273.5$ MPa	$n_1 = 76{,}670$ cycles $n_2 = 34{,}761$ cycles $n_3 = 5{,}366$ cycles $n_4 = 1{,}111$ cycles	$\sum n_i = 117{,}908$ cycles $\sum \dfrac{n_i}{N_{fi}} = 4 \times 0.05 = 0.2$
(diagram)	$\sigma_1 = 0.7\,X_T = 273.5$ MPa $\sigma_2 = 0.6\,X_T = 234.4$ MPa $\sigma_3 = 0.4\,X_T = 156.3$ MPa $\sigma_4 = 0.3\,X_T = 117.2$ MPa	$n_1 = 1{,}111$ cycles $n_2 = 5{,}366$ cycles $n_3 = 34{,}761$ cycles $n_4 = 76{,}670$ cycles	$\sum n_i = 117{,}908$ cycles $\sum \dfrac{n_i}{N_{fi}} = 4 \times 0.05 = 0.2$

Figure 10 and Figure 11 show the simulated cycle history of damage and fatigue failure index for the high-low and low-high order of the four-unit block load sequence, respectively. Indeed, as observed by Adam et al. [3], the fatigue life for the high-low order ($N_f = 354{,}651$ cycles) is predicted considerably shorter than for the low-high order ($N_f = 470{,}522$ cycles), and conform with the observations by Adam et al., failure occurs for both cases at the start of a new block with the highest stress level. It may be noticed that the Palmgren-Miner's sum with these simulations is smaller than 1.0 for both load order sequences, which was not the case with the four-unit block loading experiments by Adam et al. However, here the applied stress levels vary between $0.3 \times X_T$ and $0.7 \times X_T$, while the applied stress levels for the experiments by Adams et al. were only between $0.60 \times X_T$ and $0.78 \times X_T$.
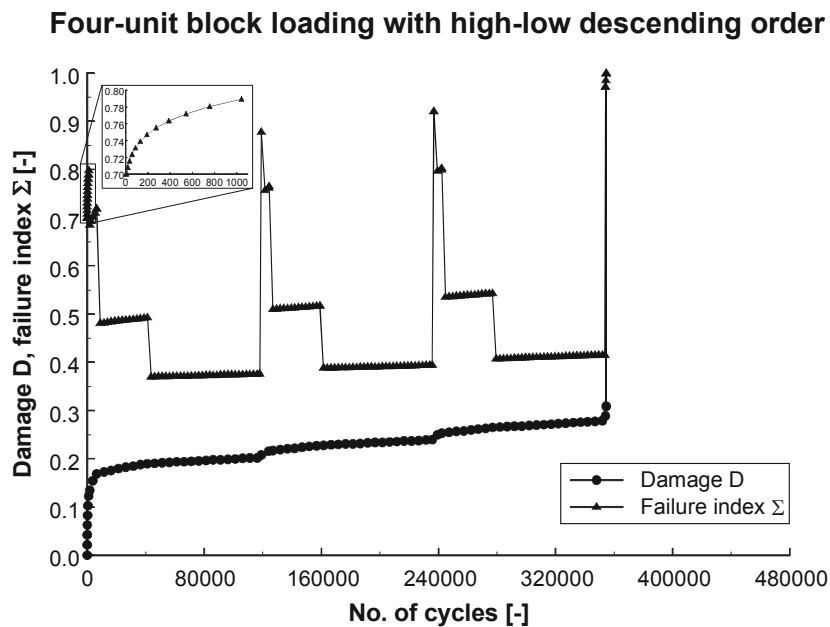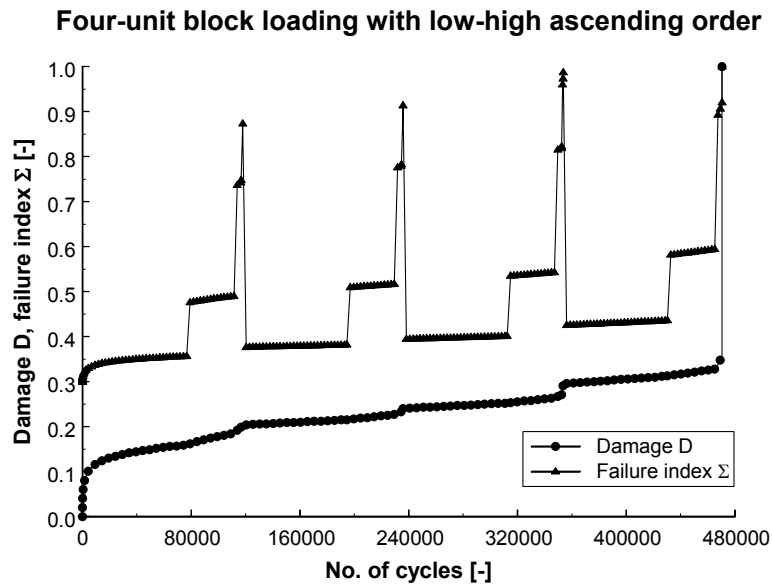

Four-unit block loading with high-low descending order

Figure 10   **Cycle history of damage and fatigue failure index for high-low order of the four-unit block load sequence.**

Four-unit block loading with low-high ascending order

Figure 11   Cycle history of damage and fatigue failure index for low-high order of the four-unit block load sequence.

Adam et al. [3] concluded from their experiments that a low initial stress appears more beneficial than a high initial stress. However, in the authors' opinion, the major difference in both loading sequences lies in the fact that the largest transition from a low to a high stress level is more damaging for the high-low descending order than for the low-high ascending order (see schematic drawing in Table 3). With the high-low descending order, there is a brutal change of the stress level from $0.3 \times X_T$ to $0.7 \times X_T$, while this difference is accumulated more gradually with the low-high ascending order.

In the authors' opinion, it may therefore be concluded that there is no general statement that low-high load sequences are more or less damaging than high-low load sequences. It strongly depends on the transitions from low to high stress level, and their number of appearance ("cycle mix effect"). Moreover, the time during fatigue life at which these transitions occur, is important as well, because the increase of the effective stress $\tilde{\sigma}$ (and hence the failure index $\Sigma(\sigma, D)$) is dependent on the present damage D. Hence the present simulations provide strong evidence that due to the stiffness degradation during fatigue life, the loading history should be fully simulated to correctly take into account all load sequence effects. Besides, once the fatigue damage model has been elaborated, no experimental damage accumulation rules or "cycle mix factors" should be applied, since the damage evolution under each stress level is predicted by the damage growth rate equation dD/dN.

CONCLUSIONS

From a literature survey, it has been concluded that the opinions on the load sequence effect are strongly divided. Some of the experimental fatigue testing programmes support the opinion that a low-high load sequence is more damaging than a high-low load sequence, while other fatigue experiments seem to prove the contrary.

A phenomenological residual stiffness model has been proposed, which predicts the damage development in terms of stiffness degradation through the state variable $D = 1 - E/E_0$. A failure criterion has been incorporated in the model by a different interpretation of the static

Tsai-Wu failure criterion. This fatigue damage model has then been used to simulate the effect of block loading on bending fatigue tests with glass/epoxy composites. Finally, numerical simulations on block loading, the "cycle mix effect" and four-unit block loading sequences have been performed for tensile fatigue loading. These simulations have qualitatively shown that there is no general statement possible on the damaging effect of low-high and high-low load sequences. The most damaging effect is the (frequent) transition from a low to a high stress level, and it strongly depends on the number of these transitions and the present damage whether a low-high or a high-low load sequence is the most damaging one.

REFERENCES

[1]   Schutz, D. (1981). Variable amplitude fatigue testing. In: AGARD Lecture Series No. 118. Fatigue test methodology, pp. 4.1-4.31

[2]   Miner, M.A. (1945). Cumulative damage in fatigue. Journal of Applied Mechanics, 67, A159-A164.

[3]   Adam, T., Gathercole, N., Reiter, H. and Harris, B. (1994). Life prediction for fatigue of T800/5245 carbon-fibre composites: II. Variable-amplitude loading. International Journal of Fatigue, 16(8), 533-547.

[4]   Fatemi, A. and Yang, L. (1998). Cumulative fatigue damage and life prediction theories: a survey of the state of the art for homogeneous materials. International Journal of Fatigue, 20(1), 9-34.

[5]   Hashin, Z. (1985). Cumulative damage theory for composite materials: residual life and residual strength methods. Composites Science and Technology, 23, 1-19.

[6]   Bartley-Cho, J., Lim, S.G., Hahn, H.T. and Shyprykevich, P. (1998). Damage accumulation in quasi-isotropic graphite/epoxy laminates under constant-amplitude fatigue and block loading. Composites Science and Technology, 58, 1535-1547.

[7]   Gamstedt, E.K. and Sjogren, B.A. (2000). On the sequence effect in block amplitude loading of cross-ply composite laminates. In: Proceedings of the Second International Conference on Fatigue of Composites. 4-7 June 2000, Williamsburg, pp. 9.3.

[8]   Broutman, L.J. and Sahu, S. (1972). A new theory to predict cumulative fatigue damage in fiberglass reinforced plastics. In: Composite materials: Testing and design (Second conference), ASTM STP 497. Philadelphia, ASTM, pp. 170-188.

[9]   Yang, J.N. and Jones, D.L. (1981). Load sequence effects on the fatigue of unnotched composite materials. In : Lauraitis, K.N. (ed.). Fatigue of fibrous composite materials. ASTM STP 723. Philadelphia, American Society for Testing and Materials, pp. 213-232.

[10]   Schaff, J.R. and Davidson, B.D. (1997). Life prediction methodology for composite structures. Part I - Constant amplitude and two-stress level fatigue. Journal of Composite Materials, 31(2), 128-157.

[11]   Schaff, J.R. and Davidson, B.D. (1997). Life prediction methodology for composite structures. Part II - Spectrum fatigue. Journal of Composite Materials, 31(2), 158-181.

[12]   Farrow, I.R. (1989). Damage accumulation and degradation of composite laminates under aircraft service loading : assessment and prediction. Volumes I and II. Cranfield Institute of Technology, Ph.D. Thesis

[13]   Whitworth, H.A. (1990). Cumulative damage in composites. Journal of Engineering Materials and Technology, 112, 358-361.

[14]   Lee, C.-H. and Jen, M.-H.R. (2000). Fatigue response and modelling of variable stress amplitude and frequency in AS-4/PEEK composite laminates. Part 1: Experiments. Journal of Composite Materials, 34(11), 906-929.

[15]   Lee, C.-H. and Jen, M.-H.R. (2000). Fatigue response and modelling of variable stress amplitude and frequency in AS-4/PEEK composite laminates. Part 2: Analysis and formulation. Journal of Composite Materials, 34(11), 930-953.

[16]   Hwang, W. and Han, K.S. (1986). Cumulative damage models and multi-stress fatigue life prediction. Journal of Composite Materials, 20, 125-153.

[17]   Han, K.S. and Hamdi, M. (1983). Fatigue life scattering of RP/C. 38th Annual RP/CI Conference, SPI.

[18]   Gathercole, N., Reiter, H., Adam, T. and Harris, B. (1994). Life prediction for fatigue of T800/5245 carbon-fibre composites: I. Constant-amplitude loading. International Journal of Fatigue, 16(8), 523-532.

[19]   Van Paepegem, W. and Degrieck, J. (2001). New coupled coupled approach of residual stiffness and strength for fatigue of fibre-reinforced composites. Accepted for presentation at ICCE/8.

[20]   Schulte, K. (1984). Stiffness reduction and development of longitudinal cracks during fatigue loading of composite laminates. In : Cardon, A.H. and Verchery, G. (eds.). Mechanical characterisation of load bearing fibre composite laminates. Proceedings of the European Mechanics Colloquium 182, 29-31 August 1984, Brussels, Belgium, Elsevier, pp. 36-54.

[21]   Highsmith, A.L. and Reifsnider, K.L. (1982). Stiffness-reduction mechanisms in composite laminates. In : Reifsnider, K.L. (ed.). Damage in composite materials. ASTM STP 775. American Society for Testing and Materials, pp. 103-117.

[22]   Masters, J.E. and Reifsnider, K.L. (1982). An investigation of cumulative damage development in quasi-isotropic graphite/epoxy laminates. In : Reifsnider, K.L. (ed.). Damage in composite materials. ASTM STP 775. American Society for Testing and Materials, pp. 40-62.

[23]   Van Paepegem, W. and Degrieck, J. (2000). Numerical modelling of fatigue degradation of fibre-reinforced composite materials. In: Topping, B.H.V. (ed.). Proceedings of the Fifth International Conference on Computational Structures Technology. Volume F: Computational Techniques for Materials, Composites and Composite Structures, Leuven, 6-8 September 2000, Civil-Comp Press, pp. 319-326.

[24]   Sol, H. and de Wilde, W.P. (1988). Identification of elastic properties of composite materials using resonant frequencies. In : Brebbia, C.A., de Wilde, W.P. and Blain, W.R. (eds.). Proceedings of the International Conference "Computer Aided Design in Composite Material Technology", Southampton, 1988, Springer-Verlag, pp. 273-280.

[25]   Sol, H. (1990). Identification of the complex moduli of composite materials by a mixed numerical/experimental method. In : de Wilde, W.P. and Blain, W.R. (eds.). Proceedings of the second International Conference on Computer Aided Design in Composite Material Technology, Brussels, 25-27 April 1990, Springer-Verlag, pp. 267-279.